Marine emissions and trade winds control the atmospheric nitrous oxide in the Galapagos Islands

Timur Cinay[1], Dickon Young[2], Nazaret Narváez Jimenez[3], Cristina Vintimilla-Palacios[3], Ariel Pila Alonso[3], Paul B. Krummel[4], William Vizuete[5], and Andrew R. Babbin[1]

[1]Department of Earth, Atmospheric & Planetary Sciences, Massachusetts Institute of Technology, Cambridge, MA, USA
[2]School of Chemistry, University of Bristol, Bristol, UK
[3]Galapagos Science Center (GSC), Universidad San Francisco de Quito (USFQ) and UNC-Chapel Hill, Puerto Baquerizo Moreno, Galapagos, Ecuador
[4]Centre for Australian Weather and Climate Research, CSIRO Environment, Aspendale, Victoria, Australia
[5]Department of Environmental Sciences Engineering, University of North Carolina, Chapel Hill, NC, USA

Correspondence: Timur Cinay (tcinay@mit.edu) and Andrew R. Babbin (babbin@mit.edu)
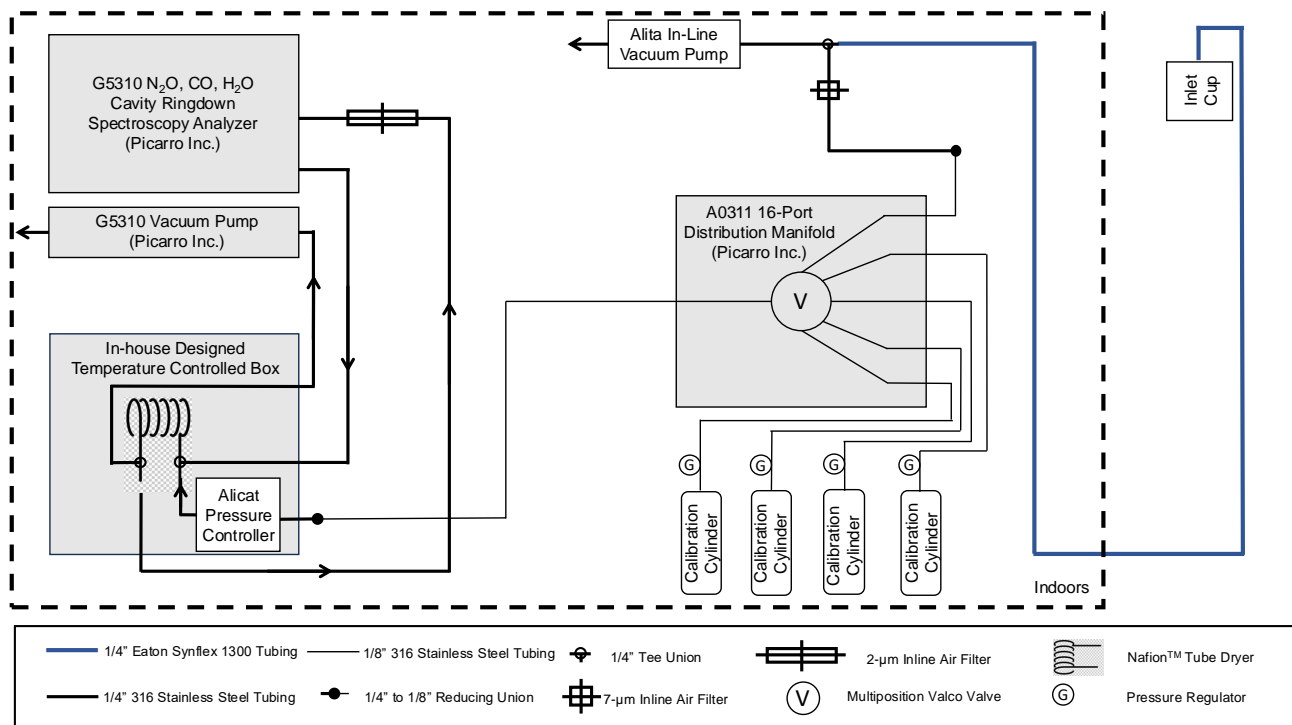
Figure S1. Air flow diagram of the setup at the Galapagos Emissions Monitoring Station for measuring atmospheric mole fraction of N_2O and CO. Dashed lines indicate the indoor space where the instruments are housed. Specific components are listed in the legend.
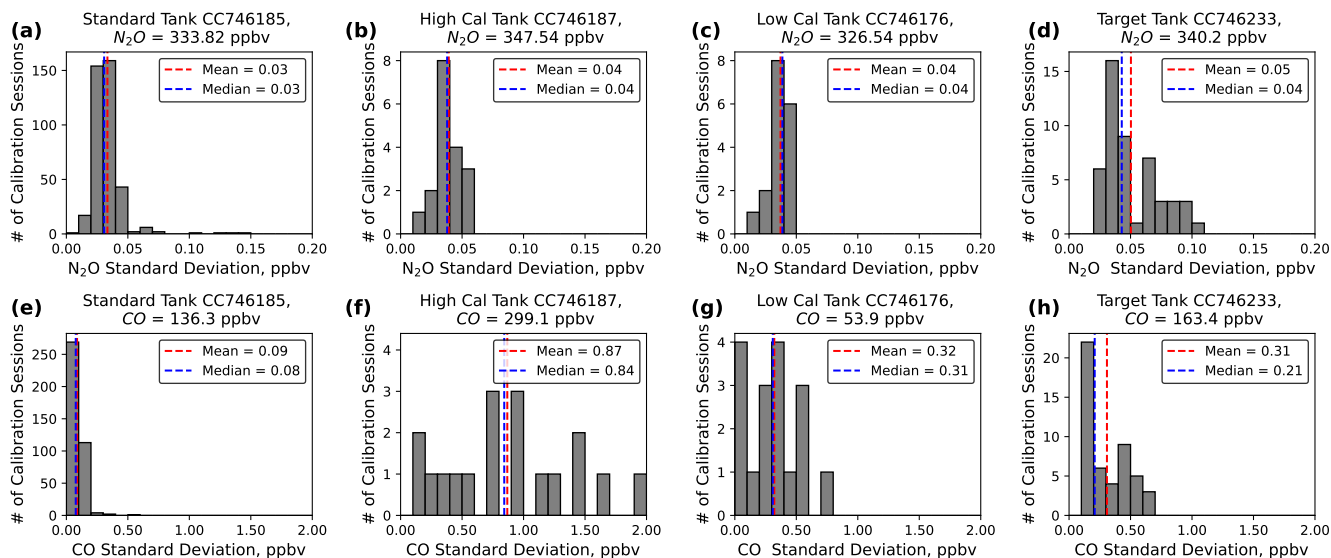
Figure S2. Repeatability analysis for N_2O and CO measurements at the Galapagos Emissions Monitoring Station. In the subplots, each column represents a singular calibration tank, whereas each row represents the measured species, i.e., N_2O or CO. In each subplot, a histogram of the standard deviation of each calibration session is plotted with the mean and the median marked by red and blue dotted lines, respectively. The repeatability is then calculated by averaging all the mean values for each tank and species.
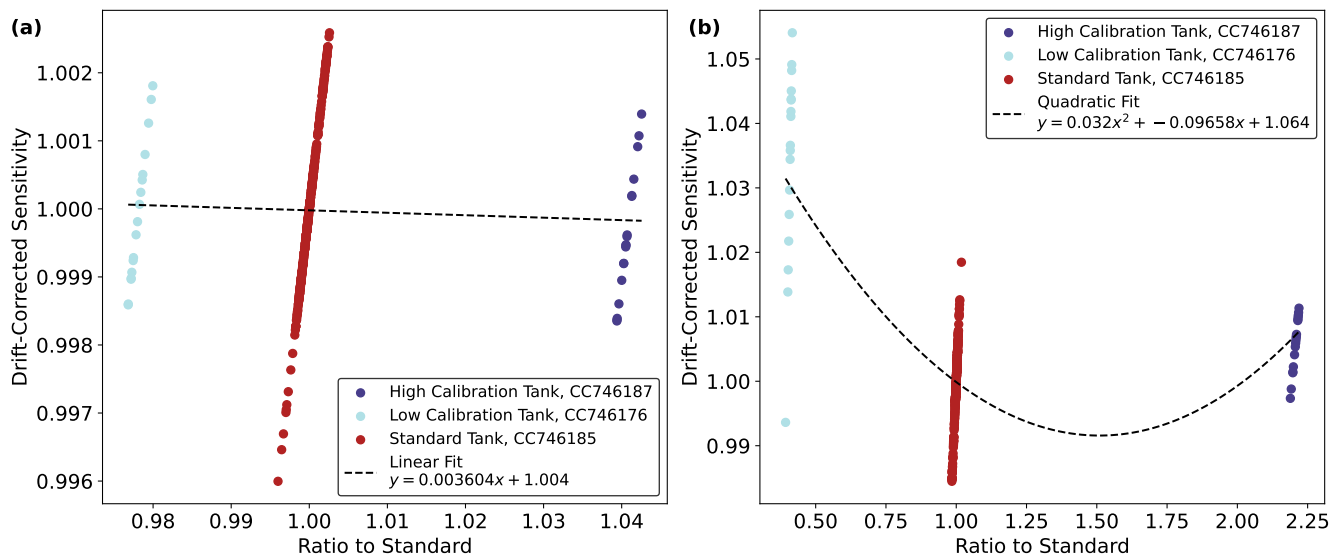
Figure S3. Drift-corrected sensitivity vs. ratio to standard values for three calibration tanks: (a) N_2O and (b) CO measurements. The dashed black line indicates the equation fit for non-linearity correction calculations.
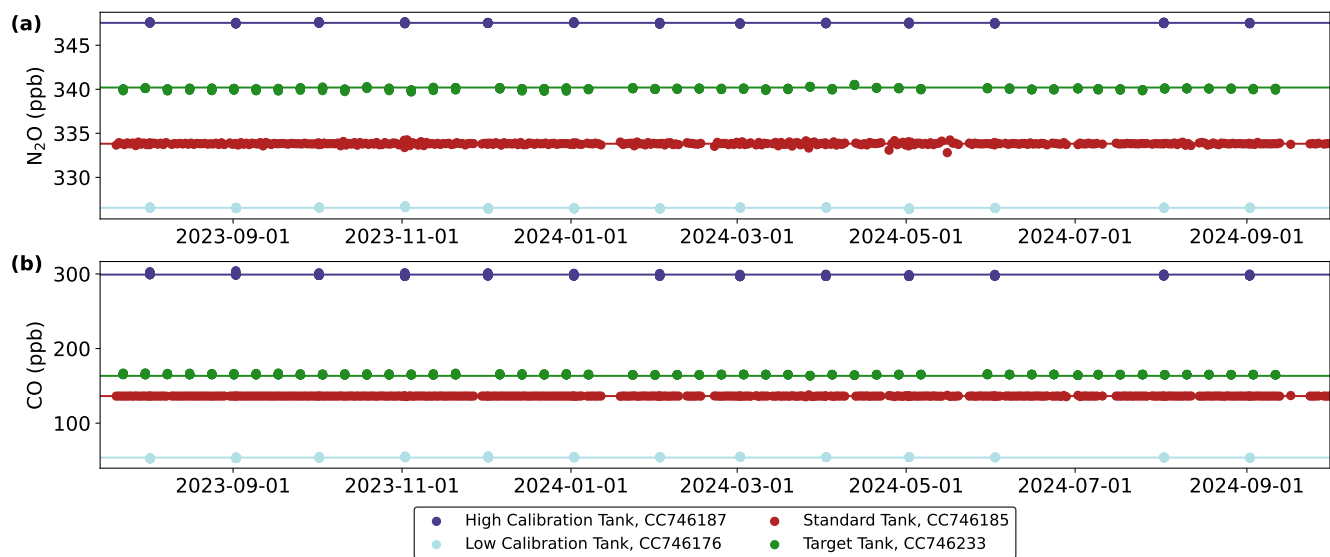
Figure S4. Reported mole fraction values of (a) N$_2$O and (b) CO measured in the calibration tanks. The reported values are drift-corrected and calibrated after the measurement of N$_2$O and CO dry mole fractions.
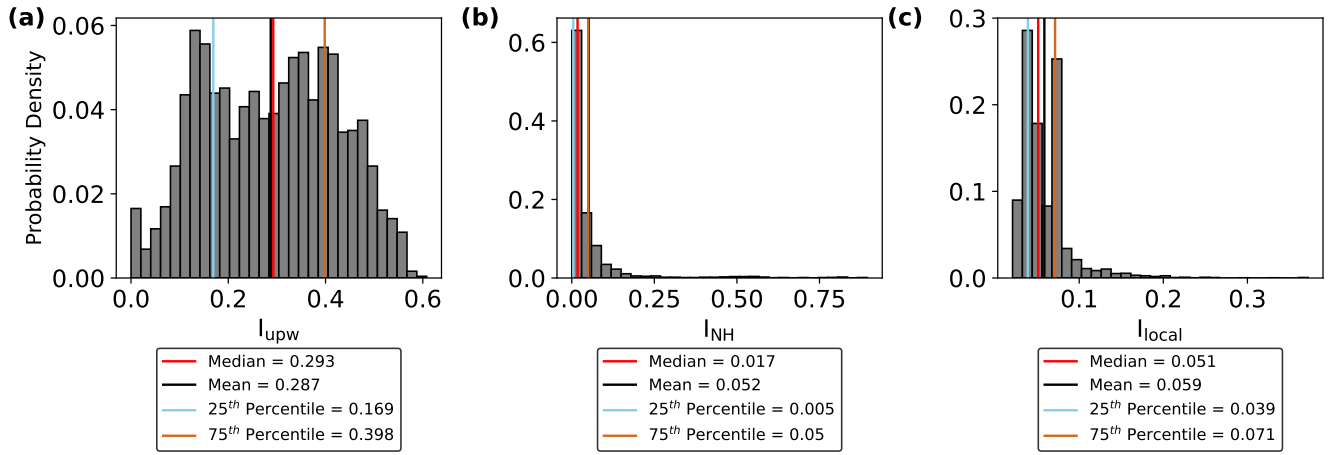
Figure S5. Histograms of regional influence metrics for the (a) Peruvian and Chilean upwelling systems (I_{upw}), (b) Northern Hemisphere (I_{NH}), and (c) a local 3-by-3 grid centered on the GEMS region (I_{local}) from July 2023 to June 2024. The mean, median, 25th, and 75th percentiles are marked by straight lines.
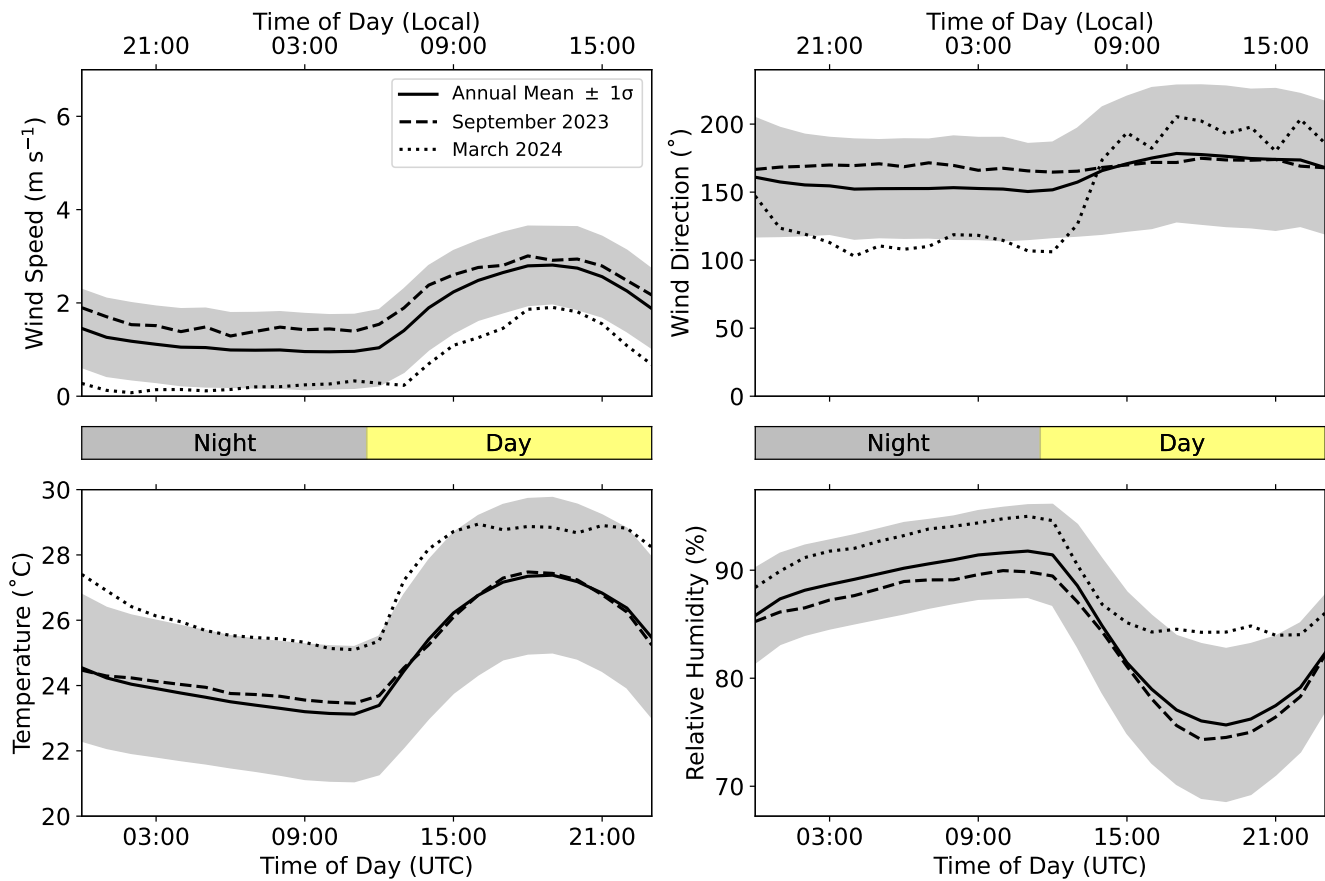
Figure S6. Diurnal cycle of (a) wind speed, (b) wind direction, (c) temperature, and (d) relative humidity measured at the Galapagos Science Center Weather Station. Solid lines represent the hourly mean annually, whereas dashed and dotted lines represent the monthly means for September 2023 and March 2024, respectively. The dark shaded area represents the one standard deviation range of the annual observations
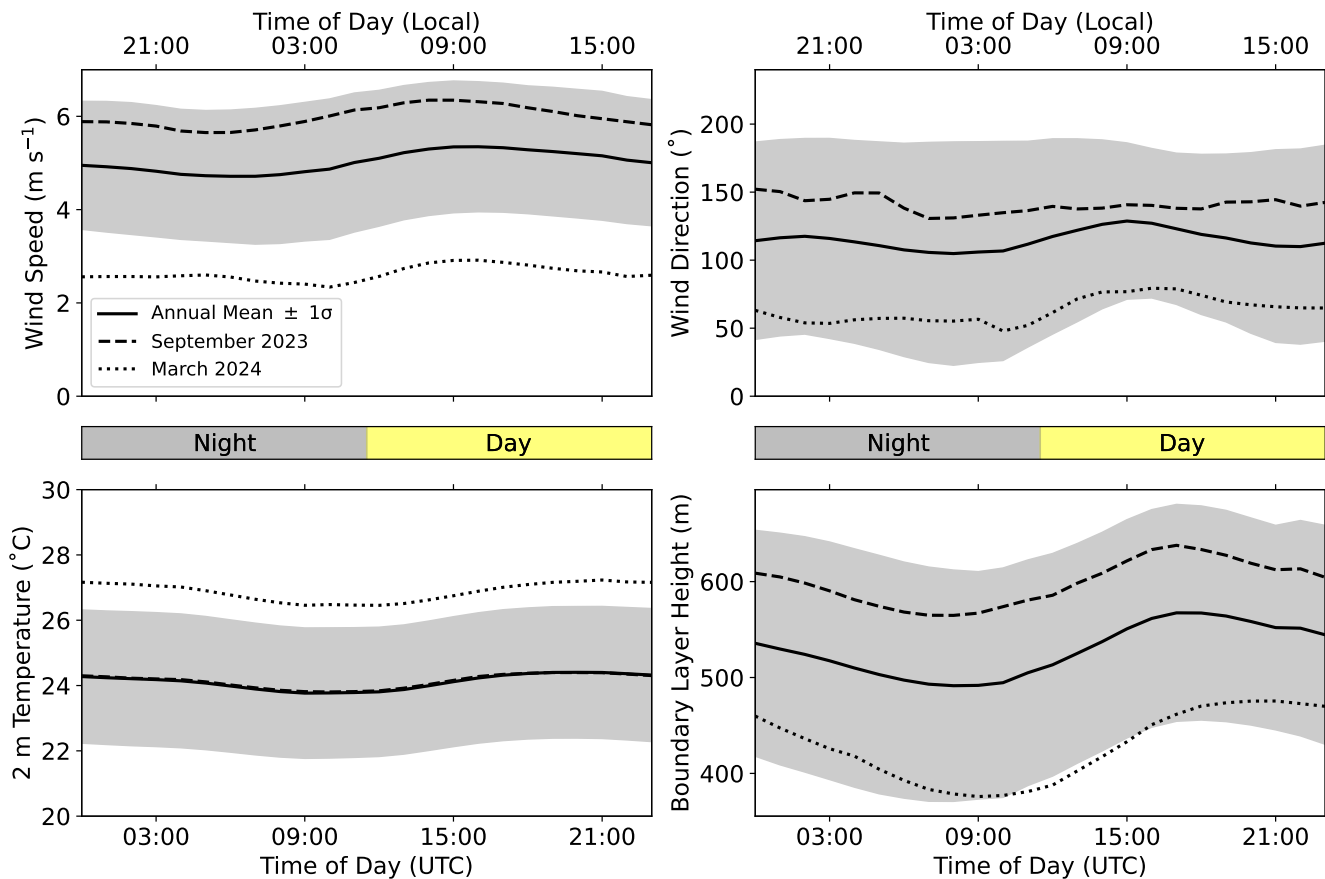
Figure S7. Diurnal cycle of (a) wind speed, (b) wind direction, (c) 2 m temperature, and (d) boundary layer height reported by ERA5 reanalysis product obtained from ECMWF for the grid cell in which the Galapagos Emissions Monitoring Station is located. Solid lines represent the hourly mean annually, whereas dashed and dotted lines represent the monthly means for September 2023 and March 2024, respectively. The dark shaded area represents the one standard deviation range of the annual observations.